Structure–Activity Study on the Quinone/Quinone Methide Chemistry of Flavonoids

ARTICLE *in* CHEMICAL RESEARCH IN TOXICOLOGY · MAY 2001

Impact Factor: 3.53 · DOI: 10.1021/tx000216e · Source: PubMed

6 AUTHORS, INCLUDING:

Hanem Awad
National Research Center, Egypt
44 PUBLICATIONS **763** CITATIONS
SEE PROFILE

Sjef Boeren
Wageningen University
124 PUBLICATIONS **3,881** CITATIONS
SEE PROFILE

Peter J van Bladeren
Nestlé S.A.
422 PUBLICATIONS **10,367** CITATIONS
SEE PROFILE

J.J.M. Vervoort
Wageningen University
398 PUBLICATIONS **7,795** CITATIONS
SEE PROFILE

Structure−Activity Study on the Quinone/Quinone Methide Chemistry of Flavonoids

Hanem M. Awad,[†,‡] Marelle G. Boersma,[†] Sjef Boeren,[†] Peter J. van Bladeren,[§,||] Jacques Vervoort,[†] and Ivonne M. C. M. Rietjens*[,†,§,||]

Laboratory of Biochemistry, Wageningen University, Dreijenlaan 3, 6703 HA Wageningen, The Netherlands, Department of Tanning Materials & Proteins, National Research Centre, 12622 Dokki, Cairo, Egypt, Division of Toxicology, Wageningen University, Tuinlaan 5, 6703 HE Wageningen, The Netherlands, and TNO/WU Centre for Food Toxicology, P.O. Box 8000, 6700 EA Wageningen, The Netherlands

Received October 11, 2000

A structure−activity study on the quinone/quinone methide chemistry of a series of 3′,4′-dihydroxyflavonoids was performed. Using the glutathione trapping method followed by HPLC, ^{1}H NMR, MALDI-TOF, and LC/MS analysis to identify the glutathionyl adducts, the chemical behavior of the quinones/quinone methides of the different flavonoids could be deduced. The nature and type of mono- and diglutathionyl adducts formed from quercetin, taxifolin, luteolin, fisetin, and 3,3′,4′-trihydroxyflavone show how several structural elements influence the quinone/quinone methide chemistry of flavonoids. In line with previous findings, glutathionyl adduct formation for quercetin occurs at positions C6 and C8 of the A ring, due to the involvement of quinone methide-type intermediates. Elimination of the possibilities for efficient quinone methide formation by (i) the absence of the C3−OH group (luteolin), (ii) the absence of the C2═C3 double bond (taxifolin), or (iii) the absence of the C5−OH group (3,3′,4′-trihydroxyflavone) results in glutathionyl adduct formation at the B ring due to involvement of the *o*-quinone isomer of the oxidized flavonoid. The extent of di- versus monoglutathionyl adduct formation was shown to depend on the ease of oxidation of the monoadduct as compared to the parent flavonoid. Finally, unexpected results obtained with fisetin provide new insight into the quinone/quinone methide chemistry of flavonoids. The regioselectivity and nature of the quinone adducts that formed appear to be dependent on pH. At pH values above the pK_a for quinone protonation, glutathionyl adduct formation proceeds at the A or B ring following expected quinone/quinone methide isomerization patterns. However, decreasing the pH below this pK_a results in a competing pathway in which glutathionyl adduct formation occurs in the C ring of the flavonoid, which is preceded by protonation of the quinone and accompanied by H_2O adduct formation, also in the C ring of the flavonoid. All together, the data presented in this study confirm that quinone/quinone methide chemistry can be far from straightforward, but the study provides significant new data revealing an important pH dependence for the chemical behavior of this important class of electrophiles.

Introduction

Flavonoids, which are widely distributed in green vegetables, fresh fruits, nuts, seeds, tea, olive oil, and red wine (*1*, *2*), have recently been identified as a major cancer-preventive component of our diet because of their antioxidative, oxygen radical scavenging, and anti-inflammatory activities (*2*−*5*). There are also claims that they are antiartherosclerotic (*6*, *7*) and, in addition, may provide beneficial health effects in aging (*1*, *4*). However, depending on the concentration and OH substituent pattern, these polyphenolic compounds can also act as pro-oxidants (*8*−*10*). This holds true especially for flavonoids containing a catechol-like 3′,4′-dihydroxy substituent pattern in their B ring as in, for example, quercetin (Table 1) (*9*, *10*). This catechol moiety provides possibilities for efficient autoxidation and/or enzymatic one- as well as two-electron oxidation of the flavonoid, all resulting in the formation of semiquinone- and quinone-type metabolites. These semiquinone- and quinone-type metabolites may act as electrophiles binding to cellular macromolecules and may also result in the production of reactive oxygen species through redox cycling (*11*, *12*). The ability of quinones to redox cycle and create reactive oxygen species and their ability to form covalent adducts with cellular macromolecules are the bases for their potential harmful pro-oxidative effect. The mutagenicity of quercetin is an example of a harmful effect ascribed to the formation of such alkylating quinone-type metabolites (*2*, *13*, *14*). Furthermore, the carcinogenic effects of estrogens and polycyclic aromatic hydrocarbons have recently also been linked to the formation of catechol-type metabolites which subsequently (auto)-oxidize to reactive quinones, resulting in similar toxic mechanisms (*11*−*13*, *15*).

* To whom correspondence should be addressed: Laboratory of Biochemistry, Wageningen University, Dreijenlaan 3, 6703 HA Wageningen, The Netherlands. Phone: 31-0317-482868. Fax: 31-0317-484801. E-mail: ivonne.rietjens@P450.bc.wau.nl.

[†] Laboratory of Biochemistry, Wageningen University.

[‡] National Research Centre.

[§] Division of Toxicology, Wageningen University.

[||] TNO/WU Centre for Food Toxicology.

10.1021/tx000216e CCC: $20.00
Published on Web 03/27/2001

Table 1. Substituent Patterns and Structure Characteristics of the Flavonoids of Importance for the Study Presented Here

	3′-OH	4′-OH	3-OH	C4═O	5-OH	7-OH	C2═C3
quercetin	+	+	+	+	+	+	+
taxifolin	+	+	+	+	+	+	−
luteolin	+	+	−	+	+	+	+
fisetin	+	+	+	+	−	+	+
3,3′,4′-trihydroxyflavone	+	+	+	+	−	−	+

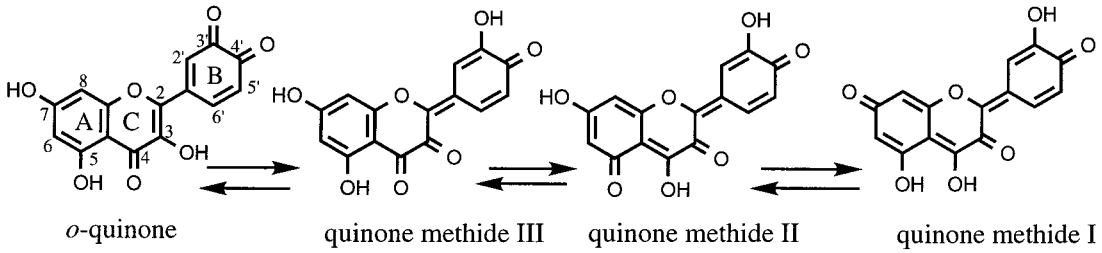

Figure 1. Quinone/quinone methide isomerization of quercetin.

Previous studies that included incubating flavonoids with peroxidases in the presence of GSH[1] have indicated the capacity of GSH to scavenge the flavonoid semiquinone radical, thereby regenerating the flavonoid and generating oxidized GSH and reactive oxygen species leading to toxicity (*10*, *16*). This reaction appeared to be especially efficient for flavones and flavanones containing a phenol-type substituent pattern in their B ring (*16*, *17*). The GSH oxidizing pro-oxidant activity of this type of flavone and flavanone seemed to partly correlate with the high one-electron redox potential of the corresponding phenoxyl radicals (*16*, *18*). Flavonoids containing a catechol-type substituent pattern in their B ring did not co-oxidize GSH when oxidized by horseradish peroxidase (HRP), presumably because of their lower one-electron redox potentials, although it was observed that some GSH depletion did occur without oxygen uptake or GSSG formation (*16*, *18*). Thus, the absence of GSH oxidation upon HRP-catalyzed oxidation of quercetin may be due to GSH conjugate formation of the quercetin quinone/quinone methide. Using the glutathione trapping method for scavenging the reactive and unstable quinoid-type metabolites (*19*−*21*), we recently identified these glutathione conjugates of the quinoid-type metabolite of quercetin. The same adducts were formed upon one- or two-electron oxidation of quercetin catalyzed by HRP (*22*) or tyrosinase (*23*), respectively. Surprisingly, glutathione addition to the quinoid metabolite of quercetin, in both cases, occurred in the A ring instead of in the catechol-containing B ring. The formation of 6-glutathionyl- and 8-glutathionylquercetin pointed at the efficient isomerization of the *o*-quinone quercetin metabolite to quercetin quinone methide isomers (Figure 1). It can be foreseen that this nonenzymatic isomerization of quercetin *o*-quinone to its quinone methides will depend on the structure of the polyphenol compound. Therefore, the objective of this study was to further investigate the quinone/quinone methide chemistry of a series of 3′,4′-dihydroxyflavones using the GSH trapping method. Special emphasis was placed on the regioselectivity of the GSH conjugation and on the structural requirements in the flavonoids necessary for quinone/quinone methide isomerization, taking into consideration the role of especially the C2═C3 double bond, the C3−OH group, and the C5− and C7−hydroxyl moieties of quercetin. Thus, the quinone/quinone methide chemistry of taxifolin, luteolin, fisetin, and 3,3′,4′-trihydroxyflavone was investigated and compared to that previously elucidated for quercetin.

[1] Abbreviations: MALDI-TOF-MS, matrix-assisted laser desorption ionization time-of-flight mass spectrometry; GSH, glutathione; HRP, horseradish peroxidase.

Materials and Methods

Materials. Quercetin (toxic, exhibits mutagenic activity) was obtained from Acros Organics. Fisetin (irritant) was from Aldrich (Steinheim, Germany). Luteolin and 3,3′,4′-trihydroxyflavone were from Indofine. Taxifolin was obtained from ICN Biomedicals Inc. Horseradish peroxidase was obtained from Boehringer (Mannheim, Germany). Glutathione, reduced form, was purchased from Sigma (St. Louis, MO). All substrates were 98−99% pure. Hydrogen peroxide, potassium hydrogen phosphate, potassium dihydrogen phosphate, and trifluoroacetic acid were purchased from Merck (Darmstadt, Germany). Deuterium oxide was obtained from ARC Laboratories (Amsterdam, The Netherlands). Acetonitrile and methanol were HPLC grade from Lab-Scan, Analytical Sciences (Dublin, Ireland).

Incubation of Flavonoids with Glutathione. To a starting solution of flavonoid (final concentration of 150 μM added from a 10 mM stock solution in methanol) in 25 mM potassium phosphate (pH 7.0) containing glutathione (final concentration of 1.0 mM) was added HRP to a final concentration of 0.1 μM, followed by addition of H_2O_2 (final concentration of 200 μM added from a 20 mM stock solution in water). Upon incubation for 8 min at 25 °C, the incubation mixture was analyzed by HPLC.

pH Dependence for Incubation of Fisetin with Glutathione. To a starting solution of fisetin (final concentration of 150 μM added from a 10 mM stock solution in methanol) in 25 mM buffer with a pH varying between 3.5 and 11.0 [prepared according to the literature (*24*−*26*)], containing glutathione (final concentration of 1.0 mM), was added HRP to a final concentration of 0.1 μM, followed by addition of H_2O_2 (final concentration of 200 μM added from a 20 mM stock solution in water). Upon incubation for 8 min at 25 °C, the incubation mixture was analyzed by HPLC.

Analytical High-Performance Liquid Chromatography. HPLC was performed with a Waters M600 liquid chromatography system. Analytical separations were achieved using an Alltima C18 column (4.6 mm × 150 mm) (Alltech, Breda, The Netherlands). The column was eluted at 0.7 mL/min with water containing 0.1% (v/v) trifluoroacetic acid. A linear gradient from 0 to 30% acetonitrile over the course of 18 min was applied, followed by 2 min isocratic elution with 30% acetonitrile. Hereafter, a linear gradient from 30 to 100% acetonitrile was

used over the course of 10 min. The percentage of acetonitrile was kept at 100% for an additional 10 min. An injection loop of 10 μL was used. Detection was carried out with a Waters 996 photodiode array detector measuring spectra between 200 and 450 nm. The chromatograms presented here are based on detection at 290 nm. Product peaks were collected and freeze-dried for further analysis by ^{1}H NMR, MALDI-TOF, and LC/MS analysis. Freeze-dried samples were dissolved in 25 mM potassium phosphate (pH 7.0), made with deuterated water when samples were used for ^{1}H NMR analysis.

NMR Measurements. ^{1}H NMR measurements were performed on a Bruker DPX 400 or Bruker AMX 500 spectrometer. A 1.5 s presaturation delay was used, along with a 70° pulse angle and a 2.2 s acquisition time (7575 Hz sweep width, 32K data points, 7 °C). The data were processed using an exponential multiplication of 0.5 or 1.0 Hz and zero filling to 64K data points. Resonances are reported relative to HDO at 4.79 ppm. ^{13}C NMR measurements were performed in a deuterated methanol/D_2O mixture at 15 °C with a dedicated 5 mm ^{13}C NMR probe (32 000 Hz sweep width, 65K data points, 28 000 scans).

Liquid Chromatography/Mass Spectrometry. LC/MS analysis was performed to further characterize the peaks in the HPLC elution pattern that could not be identified as one of the reference compounds. An injection volume of 10 μL from the incubation mixture or from the purified metabolite dissolved in potassium phosphate (pH 7.0) was used, and separation of the products was achieved on a 150 mm × 4.6 mm Alltima C18 column (Alltech). A gradient from 10 to 30% acetonitrile in water containing 0.1% (v/v) trifluoroacetic acid was applied at a flow rate of 0.7 mL/min over the course of 13 min. The percentage of acetonitrile was kept at 30% for 2 min and then increased to 100% over the course of an additional 2 min. Mass spectrometric analysis (MAT 95 instrument, Finnigan, San Jose, CA) was performed in the positive electrospray mode using a spray voltage of 4.5 kV and a capillary temperature of 180 °C with nitrogen as the sheath and auxiliary gas.

MALDI-TOF Mass Spectrometry. A saturated solution of α-cyano-4-hydroxycinnamic acid in a 1% trifluoroacetic acid/49.5% acetonitrile/49.5% H_2O (v/v) mixture was used as the matrix solution. Freeze-dried samples were dissolved in 20% (v/v) acetonitrile in water. The dissolved samples were diluted 2−1000-fold in the matrix solution. A 1 μL volume of the sample/matrix solution was deposited directly on a welled plate, air-dried, and introduced into the mass spectrometer. Spectra were measured with a Voyager-DE spectrometer (PerSeptive Biosystems) in the positive reflector mode. The MALDI spectra were externally calibrated using bradykinin (monoisotopic at *m*/*z* 1060.57) and one matrix peak (dimeric α-cyano-4-hydroxycinnamic acid, monoisotopic at *m*/*z* 379.09).

Molecular Orbital Calculations. Molecular orbital calculations were carried out on a Silicon Graphics Indigo^2 workstation using Spartan 5.0 (Wavefunction Inc.). The semiempirical AM1 method was applied (*27*). Geometries were fully optimized. The energy of the highest occupied molecular orbital (E_{HOMO}) of the 3′,4′-dihydroxyflavonoids under investigation and their corresponding 2′-glutathionyl adducts was calculated as the parameter to quantify their ease of oxidation, because, following Koopman's theorem $-E_{HOMO}$ equals the ionization potential of a compound. In these calculations, the glutathionyl moiety can be modeled as CH_3S (*28*−*30*).

Results

HPLC Analysis of Glutathione Adducts of Flavonoids. Panels a and b of Figure 2 show the HPLC patterns of the incubation of taxifolin with HRP (0.1 and 0.2 μM, respectively) in the presence of glutathione. Using a small amount of HRP, not all taxifolin is converted and only one major metabolite peak (t_R = 21.9 min) can be detected eluting at a position different from that of the parent flavonoid. With increasing HRP concentrations, all taxifolin is converted upon incubation for 8 min and two major metabolite peaks are formed eluting with retention times of 20.1 and 21.9 min.

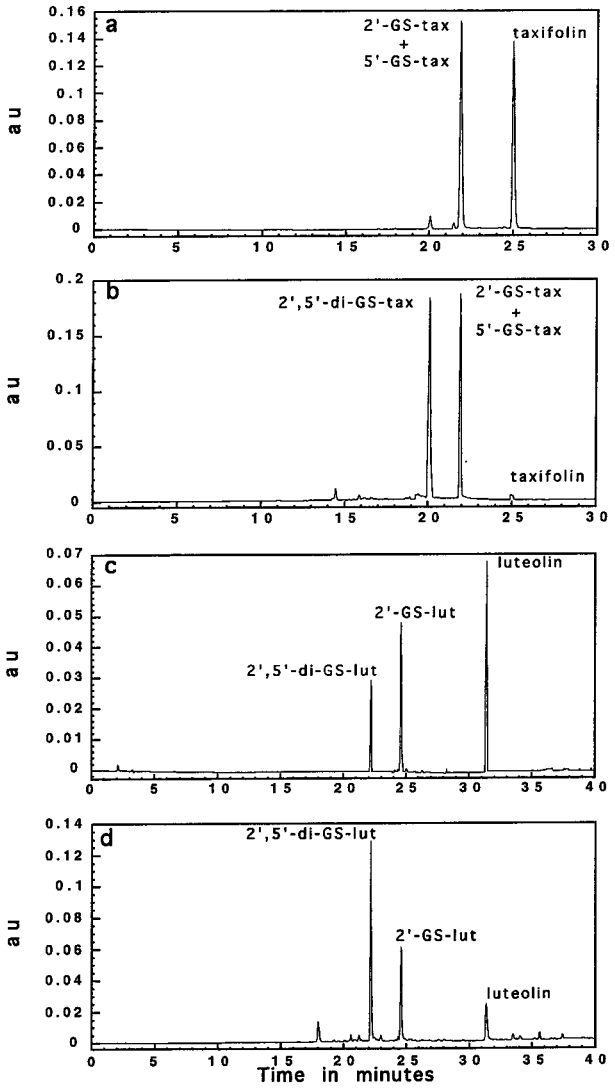

Figure 2. HPLC chromatograms of the incubations of taxifolin (a and b) and luteolin (c and d) with 0.1 and 0.2 μM HRP, respectively, in the presence of glutathione at pH 7.0.

Panels c and d of Figure 2 show the HPLC patterns of the incubation of luteolin with HRP (0.1 and 0.2 μM, respectively) in the presence of glutathione. In both cases, two metabolites can be detected eluting at a position different from that of the parent flavonoid, but the ratio between the two products appears to vary with the amount of HRP added. With a smaller amount of HRP, not all the luteolin is converted and the metabolite with a retention time of 24.6 min appears to be the one initially formed. Increasing the HRP concentration from 0.1 to 0.2 μM changes the ratio of the peak areas of the metabolites eluting at 22.2 and 24.6 min from 0.5:1 to 2:1.

Panels a and b of Figure 3 show the HPLC patterns of the incubations of 3,3′,4′-trihydroxyflavone and fisetin with HRP in the presence of glutathione. For 3,3′,4′-trihydroxyflavone, formation of one major metabolite is observed. For fisetin, two major metabolites with retention times of 15.6 and 16.5 min can be detected eluting at a position different from that of the parent flavonoid. For 3,3′,4′-trihydroxyflavone and fisetin, an increase in

Table 2. ^{1}H NMR Resonances and Coupling Constants of Taxifolin and the Glutathionyl Adducts of Taxifolin (labeled 2′-GS-tax, 5′-GS-tax, and 2′,5′-di-GS-tax)

	taxifolin		2′-GS-tax (major, 70%)		5′-GS-tax (minor, 30%)		2′,5′-di-GS-tax (t_R = 20.1 min)	
	chemical shift (ppm)	coupling constant (Hz)	chemical shift (ppm)	coupling constant (Hz)	chemical shift (ppm)	coupling constant (Hz)	chemical shift (ppm)	coupling constant (Hz)
H3	4.60 (d)	$^3J_{H3-H2} = 11.7$	4.64 (d)	$^3J_{H3-H2} = 11.6$	4.57 (d)	$^3J_{H3-H2} = 11.8$	4.45 (d)	$^3J_{H3-H2} = 11.8$
H2	4.90 (d)	$^3J_{H2-H3} = 11.7$	5.09 (d)	$^3J_{H2-H3} = 11.6$	5.26 (d)	$^3J_{H2-H3} = 11.8$	5.11 (d)	$^3J_{H2-H3} = 11.8$
H6	5.67 (d)	$^4J_{H6-H8} = 2.2$	5.71 (d)	$^4J_{H6-H8} = 2.0$	5.69 (d)	$^4J_{H6-H8} = 2.0$	5.76 (d)	$^4J_{H6-H8} = 2.4$
H8	5.75 (d)	$^4J_{H8-H6} = 2.2$	5.77 (d)	$^4J_{H8-H6} = 2.0$	5.74 (d)	$^4J_{H8-H6} = 2.0$	5.79 (d)	$^4J_{H8-H6} = 2.4$
H5′	6.80 (d)	$^3J_{H5'-H6'} = 8.2$	6.87 (d)	$^3J_{H5'-H6'} = 8.4$	–	–	–	–
H6′	6.83 (dd)	$^3J_{H6'-H5'} = 8.2$	7.16 (d)	$^3J_{H6'-H5'} = 8.4$	6.87 (d)	–	7.18 (s)	–
		$^4J_{H6'-H2'} = 2.1$		–		$^4J_{H6'-H2'} = 2.0$		–
H2′	6.93 (d)	$^4J_{H2'-H6'} = 2.1$	–	–	6.99 (d)	$^4J_{H2'-H6'} = 2.0$	–	–
Glu Hβ	–		1.79 (m)		1.84 (m)		1.82 (m)	
Glu Hγ	–		2.11 (m)		2.20 (m)		2.13 (m)	
Cys Hβ1	–		2.95 (dd)		2.96 (dd)		2.92 (dd)	
Cys Hβ2	–		3.03 (dd)		3.19 (dd)		3.24 (dd)	
Gly Hα1	–		3.32 (d)		3.38 (d)		3.34 (d)	
Gly Hα2	–		3.39 (d)		3.44 (d)		3.41 (d)	
Glu Hα	–		3.45 (m)		3.87 (m)		3.47 (m)	
Cys Hα	–		4.15 (m)		4.21 (m)		4.14 (m)	

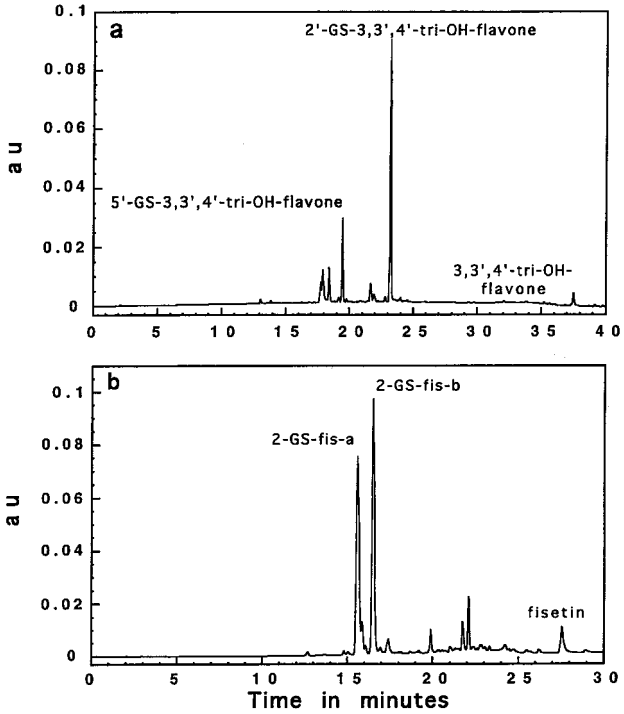

Figure 3. HPLC chromatograms of the incubations of (a) 3,3′,4′-trihydroxyflavone and (b) fisetin with HRP in the presence of glutathione at pH 7.0.

the HRP concentration from 0.1 to 0.2 μM did not modify the metabolite profile.

Identification of the Glutathionyl Flavonoid Adducts. (1) Influence of the C2═C3 Double Bond and the Results for Taxifolin. The ^{1}H NMR spectrum of the peak with a retention time of 21.9 min (Figure 2a) reveals that this peak is a mixture of two metabolites which could be separated isocraticaly using 10% acetonitrile in water containing 0.1% (v/v) trifluoroacetic acid into two metabolites showing a peak area ratio of 7:3 (HPLC chromatogram not shown). LC/MS analysis of the purified metabolites shows an M + 1 peak for both metabolites at *m*/*z* 610 (data not shown). This indicates the formation of two different monoglutathionyl adducts. Table 2 presents the ^{1}H NMR characteristics of taxifolin and these two major glutathionyl adducts formed upon incubation of taxifolin with HRP in the presence of glutathione and collected from HPLC. Comparison of the ^{1}H NMR data of the major metabolite (70%) to those of taxifolin (Table 2) (*31*, *32*) reveals the loss of especially the H2′ signal as well as the loss of the $^4J_{H2'-H6'}$ coupling of 2.1 Hz. Splitting patterns and resonances of all other aromatic protons are comparable to those of taxifolin itself. Comparison of the ^{1}H NMR data of the minor metabolite (30%) to those of taxifolin (Table 2) (*31*, *32*) reveals the loss of especially the H5′ signal as well as the loss of the $^3J_{H5'-H6'}$ coupling of 8.2 Hz. Splitting patterns and resonances of all other aromatic protons are comparable to those of taxifolin itself. In ^{1}H NMR measurements, the H2/H3 resonances of taxifolin and of the adducts are in part invisible due to peak overlap with the water resonance. However, varying the temperature from 7 to 45 °C gradually reveals these resonances, indicating the presence of the saturated C2−C3 bond in all compounds. In addition to the aromatic and the H2/H3 ^{1}H NMR resonances, the ^{1}H NMR spectra of the adducts show the ^{1}H resonances of the glutathionyl side chain (Table 2). On the basis of these ^{1}H NMR characteristics and the LC/MS data, these two metabolites can be identified as 2′-glutathionyl- and 5′-glutathionyltaxifolin.

When the HRP concentration is increased, all the parent compound was converted and an additional major metabolite was observed (Figure 2b). LC/MS analysis of the purified metabolite shows an M + 1 peak at *m*/*z* 915 (data not shown). This indicates the formation of a diglutathionyl adduct. Comparison of the ^{1}H NMR data of this additional metabolite (retention time of 20.1 min) to those of taxifolin (Table 2) (*31*, *32*) reveals the loss of especially the H2′ and H5′ signals as well as the loss of the $^4J_{H2'-H6'}$ coupling of 2.1 Hz and the $^3J_{H5'-H6'}$ coupling of 8.2 Hz. Splitting patterns and resonances of all other aromatic protons are comparable to those of taxifolin itself. On the basis of these ^{1}H NMR characteristics and LC/MS data, this metabolite can be identified as 2′,5′-diglutathionyltaxifolin.

Thus, when the absence of the C2═C3 double bond in the flavonoid prevents extension of the quinoid isomerization to ring A, the glutathionyl adducts of the oxidized flavonoid are formed in the B ring preferentially at C2′ and subsequently also at C5′.

(2) Influence of the C3−OH Group and the Results for Luteolin. Using luteolin, the influence of the absence of the C3−OH on the quinone/quinone methide

Table 3. ^{1}H NMR Resonances and Coupling Constants of Luteolin and the Two Glutathionyl Adducts of Luteolin (labeled 2′-GS-lut and 2′,5′-diGS-lut)

	luteolin		2′-GS-lut (t_R = 24.6 min)		2′,5′-diGS-lut (t_R = 22.2 min)	
	chemical shift (ppm)	coupling constant (Hz)	chemical shift (ppm)	coupling constant (Hz)	chemical shift (ppm)	coupling constant (Hz)
H6	5.99 (d)	$^4J_{H6-H8} = 1.9$	6.15 (d)	$^4J_{H6-H8} = 2.0$	6.10 (d)	$^4J_{H6-H8} = 2.0$
H8	6.26 (d)	$^4J_{H8-H6} = 1.9$	6.33 (d)	$^4J_{H8-H6} = 2.0$	6.31 (d)	$^4J_{H8-H6} = 2.0$
H3	6.40 (s)	–	6.29 (s)	–	6.26 (s)	–
H5′	6.78 (d)	$^3J_{H5'-H6'} = 8.4$	6.85 (d)	$^3J_{H5'-H6'} = 7.8$	–	–
H2′	7.25 (d)	$^4J_{H2'-H6'} = 2.1$	–	–	–	–
H6′	7.28 (dd)	$^3J_{H6'-H5'} = 8.4$ $^4J_{H6'-H2'} = 2.1$	6.99 (d)	$^3J_{H6'-H5'} = 7.8$ –	7.06 (s)	– –
Glu Hβ	–		1.73 (m)		1.66 (m)	
Glu Hγ1	–		1.86 (m)		1.80 (m)	
Glu Hγ2	–		2.06 (m)		1.92 (m)	
Cys Hβ1	–		2.80 (dd)		2.95 (m)	
Cys Hβ2	–		3.13 (dd)		3.03 (m)	
Gly Hα1	–		3.40 (d)		3.33 (d)	
Gly Hα2	–		3.42 (d)		3.33 (d)	
Glu Hα	–		3.46 (m)		3.37 (m)	
Cys Hα	–		3.71 (m)		4.19 (m)	

Table 4. ^{1}H NMR Resonances and Coupling Constants of 3,3′,4′-Trihydroxyflavone and the Glutathionyl Adducts of 3,3′,4′-Trihydroxyflavone (labeled 2′-GS-3,3′,4′-tri-OH-flavone and 5′-GS-3,3′,4′-tri-OH-flavone)

	3,3′,4′-trihydroxyflavone		2′-GS-3,3′,4′-tri-OH-flavone (major)		5′-GS-3,3′,4′-tri-OH-flavone (minor)	
	chemical shift (ppm)	coupling constant (Hz)	chemical shift (ppm)	coupling constant (Hz)	chemical shift (ppm)	coupling constant (Hz)
H5′	6.83 (d)	$^3J_{H5'-H6'} = 8.5$	6.88 (d)	$^3J_{H5'-H6'} = 8.3$	–	–
H6	7.35 (tr)	$^4J_{H6-H8} = 1.3$ $^3J_{H6-H7} = 7.1$ $^3J_{H6-H5} = 8.1$	7.32 (tr)	$^4J_{H6-H8} = 1.2$ $^3J_{H6-H7} = 7.6$ $^3J_{H6-H5} = 8.1$	7.33 (tr)	$^4J_{H6-H8} = 1.4$ $^3J_{H6-H7} = 8.6$ $^3J_{H6-H5} = 8.2$
H6′	7.58 (dd)	$^3J_{H6'-H5'} = 8.5$ $^4J_{H6'-H2'} = 1.4$	6.93 (d)	$^3J_{H6'-H5'} = 8.3$ –	7.08 (d)	– $^4J_{H6'-H2'} = 1.5$
H8	7.65 (dd)	$^4J_{H8-H6} = 1.3$ $^3J_{H8-H7} = 8.5$	7.43 (dd)	$^4J_{H8-H6} = 1.2$ $^3J_{H8-H7} = 8.7$	7.45 (dd)	$^4J_{H8-H6} = 1.4$ $^3J_{H8-H7} = 8.8$
H7	7.68 (tr)	$^4J_{H7-H5} = 1.3$ $^3J_{H7-H6} = 7.1$ $^3J_{H7-H8} = 8.5$	7.62 (tr)	$^4J_{H7-H5} = 1.7$ $^3J_{H7-H6} = 7.6$ $^3J_{H7-H8} = 8.7$	7.62 (tr)	$^4J_{H7-H5} = 1.3$ $^3J_{H7-H6} = 8.6$ $^3J_{H7-H8} = 8.8$
H2′	7.75 (d)	$^4J_{H2'-H6'} = 1.4$	–	–	7.19 (d)	$^4J_{H2'-H6'} = 1.5$
H5	8.08 (dd)	$^4J_{H5-H7} = 1.3$ $^3J_{H5-H6} = 8.1$	7.97 (dd)	$^4J_{H5-H7} = 1.7$ $^3J_{H5-H6} = 8.1$	7.97 (dd)	$^4J_{H5-H7} = 1.3$ $^3J_{H5-H6} = 8.2$
Glu Hβ	–		1.52 (m)		1.53 (m)	
Glu Hγ	–		1.85 (m)		1.84 (m)	
Cys Hβ1	–		2.68 (dd)		2.67 (dd)	
Cys Hβ2	–		3.03 (dd)		3.03 (dd)	
Gly Hα1	–		3.25 (d)		3.24 (d)	
Gly Hα2	–		3.30 (d)		3.32 (d)	
Glu Hα	–		3.40 (m)		3.41 (m)	
Cys Hα	–		3.82 (m)		3.83 (m)	

isomerization was investigated. MALDI-TOF analysis of the purified metabolites from HPLC with retention times of 24.6 and 22.2 min reveals peaks at *m*/*z* 592 and 897, respectively (data not shown). This indicates the formation of a mono- and a diglutathionyl adduct with retention times of 24.6 and 22.2 min, respectively (Figure 2c,d). The diadduct is the one with the lower retention time (22.2 min) and also the one formed in increasing amounts upon increasing the HRP concentration (Figure 2c,d).

Table 3 presents the ^{1}H NMR characteristics of these two glutathionyl adducts. Comparison of the ^{1}H NMR data of these two metabolites to those of luteolin (Table 3) (*31*−*33*) reveals the loss of especially the H2′ signal as well as the loss of the $^4J_{H2'-H6'}$ coupling of 2.1 Hz for the monoadduct. For the diglutathionyl adduct, the data indicate the loss of the H2′ and H5′ signals as well as of the $^4J_{H2'-H6'}$ coupling of 2.1 Hz and the $^3J_{H5'-H6'}$ coupling of 8.4 Hz. In addition to the aromatic ^{1}H resonances, the ^{1}H NMR spectra of both luteolin adducts show the ^{1}H resonances of the glutathionyl side chain (Table 3). On the basis of these ^{1}H NMR characteristics and the MALDI-TOF data, these two metabolites could be identified as 2′-glutathionylluteolin and 2′,5′-diglutathionylluteolin.

Thus, upon the peroxidase-mediated oxidation of luteolin, the *o*-quinone of luteolin gives rise to glutathionyl adduct formation in the B ring of luteolin initially at C2′ and subsequently also at C5′.

(3) Influence of the Hydroxyl Moieties in the A Ring and the Results for 3,3′,4′-Trihydroxyflavone and Fisetin. Using 3,3′,4′-trihydroxyflavone and fisetin (3,7,3′,4′-tetrahydroxyflavone), the influence of the two hydroxyl moieties in the A ring was investigated.

LC/MS analysis of the purified metabolites of 3,3′,4′-trihydroxyflavone shows an M + 1 peak for both the major and minor metabolite at *m*/*z* 576 (data not shown). This indicates the formation of two different monoglutathionyl adducts. Table 4 shows the ^{1}H NMR characteristics of the major metabolite of 3,3′,4′-trihydroxyflavone collected from HPLC with a retention time of 23.2 min (Figure 3a). Comparison of the ^{1}H NMR data of this metabolite to those of 3,3′,4′-trihydroxyflavone (Table 4) (*31*, *34*) reveals the loss of the H2′ signal as well as the loss of the $^4J_{H2'-H6'}$ coupling of 1.4 Hz. Splitting patterns

Table 5. ^{1}H NMR Resonances and Coupling Constants of Fisetin and the Three Glutathionyl Adducts of Fisetin (labeled 2-GS-fis-a, 2-GS-fis-b, and 2′-GS-fis)

	fisetin		2-GS-fis-a (t_R = 15.6 min)		2-GS-fis-b (t_R = 16.5 min)		2′-GS-fis (t_R = 22.1 min)	
	chemical shift (ppm)	coupling constant (Hz)	chemical shift (ppm)	coupling constant (Hz)	chemical shift (ppm)	coupling constant (Hz)	chemical shift (ppm)	coupling constant (Hz)
H8	6.81 (d)	$^4J_{H8-H6} = 1.9$	6.46 (d)	$^4J_{H8-H6} = 2.1$	6.31 (d)	$^4J_{H8-H6} = 1.9$	6.72 (d)	$^4J_{H8-H6} = 2.2$
H6	6.85 (dd)	$^3J_{H6-H5} = 8.9$	6.49 (dd)	$^3J_{H6-H5} = 8.7$	6.46 (dd)	$^3J_{H6-H5} = 8.8$	6.82 (dd)	$^3J_{H6-H5} = 8.9$
		$^4J_{H6-H8} = 1.9$		$^4J_{H6-H8} = 2.1$		$^4J_{H6-H8} = 1.9$		$^4J_{H6-H8} = 2.2$
H5′	6.94 (d)	$^3J_{H5'-H6'} = 8.5$	6.71 (d)	$^3J_{H5'-H6'} = 8.4$	6.79 (d)	$^3J_{H5'-H6'} = 8.5$	6.91 (d)	$^3J_{H5'-H6'} = 8.4$
H6′	7.61 (dd)	$^3J_{H6'-H5'} = 8.5$	7.16 (dd)	$^3J_{H6'-H5'} = 8.4$	7.21 (dd)	$^3J_{H6'-H5'} = 8.5$	6.92 (d)	$^3J_{H6'-H5'} = 8.4$
		$^4J_{H6'-H2'} = 2.1$		$^4J_{H6'-H2'} = 2.3$		$^4J_{H6'-H2'} = 2.1$		
H2′	7.69 (d)	$^4J_{H2'-H6'} = 2.1$	7.23 (d)	$^4J_{H2'-H6'} = 2.3$	7.28 (d)	$^4J_{H2'-H6'} = 2.1$	–	–
H5	7.87 (d)	$^3J_{H5-H6} = 8.9$	7.58 (d)	$^3J_{H5-H6} = 8.7$	7.59 (d)	$^3J_{H5-H6} = 8.8$	7.83 (d)	$^3J_{H5-H6} = 8.9$
Glu Hβ	–		1.81 (m)		1.70 (m)		1.60 (m)	
Glu Hγ	–		2.13 (tr)		2.01 (m)		1.90 (m)	
Cys Hβ1	–		2.35 (dd)		2.50 (dd)		2.72 (dd)	
Cys Hβ2	–		2.73 (dd)		2.65 (dd)		3.07 (dd)	
Gly Hα1	–		3.35 (d)		3.33 (d)		3.34 (d)	
Gly Hα2	–		3.40 (d)		3.43 (d)		3.34 (d)	
Glu Hα	–		3.49 (tr)		3.49 (tr)		3.37 (tr)	
Cys Hα	–		3.75 (dd)		4.04 (m)		3.82 (m)	

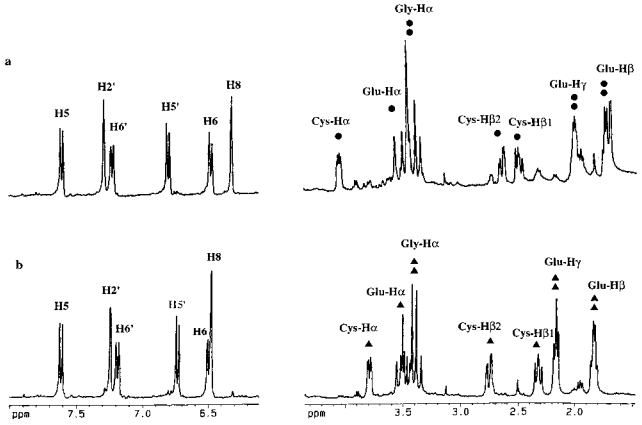

Figure 4. Aromatic and aliphatic parts of the ^{1}H NMR spectra of the two major metabolites formed in the incubation of fisetin with HRP in the presence of glutathione at pH 7.0 and eluting from the HPLC system at 15.6 (a) and 16.5 min (b) (2-glutathionylfisetin, two diastereoisomers) both measured in 25 mM potassium phosphate (pD 7.0) in D_2O.

and resonances of all other aromatic protons are comparable to those of 3,3′,4′-trihydroxyflavone itself. Comparison of the ^{1}H NMR data of the minor metabolite with a retention time of 19.4 min (Figure 3a) to those of 3,3′,4′-trihydroxyflavone (Table 4) (*31*, *34*) reveals the loss of the H5′ signal as well as the loss of the $^3J_{H5'-H6'}$ coupling of 8.5 Hz. Splitting patterns and resonances of all other aromatic protons are comparable to those of 3,3′,4′-trihydroxyflavone itself. In addition to the aromatic ^{1}H resonances, the ^{1}H NMR spectra of both adducts exhibit the ^{1}H resonances of the glutathionyl side chain. On the basis of these ^{1}H NMR characteristics and LC/MS data, the glutathionyl adducts can be identified as 2′-glutathionyl- and 5′-glutathionyl-3,3′,4′-trihydroxyflavone.

Finally, panels a and b of Figure 4 show the ^{1}H NMR spectra of the two major metabolites of fisetin collected from HPLC with retention times of 15.6 and 16.5 min (Figure 3b). For these adducts, the ^{1}H NMR spectra are presented because, in contrast to what was observed for the other flavonoid glutathionyl adducts, they reveal the retention of all the parent compound aromatic protons in both adducts. This indicates the formation of glutathionylfisetin adducts at a position other than C2′, C5′, and C6′ (B ring) or C5, C6, and C8 (A ring) (Table 5) (*31*, *34*). LC/MS analysis of the purified metabolites shows an M + 1 peak for both metabolites at *m*/*z* 610 and a second major peak at *m*/*z* 593. Because the *m*/*z* value expected for protonated monoglutathionylfisetin equals *m*/*z* 592, the observation of a peak at *m*/*z* 610 for both metabolites points at formation of monoglutathionyl adducts which contain an additional H_2O molecule. ^{13}C NMR spectra of the purified metabolites reveal formation of two sp^3 ^{13}C resonances at 92.0 and 98.4 ppm for the metabolite with a retention time of 15.6 min and at 91.6 and 95.7 ppm for the metabolite with a retention time of 16.5 min which can be assigned to the two sp^3 hybridized deshielded C atoms at C2 and C3. In addition, the ^{13}C NMR spectra of both metabolites each reveal only one resonance in the carbonyl region (at 189.0 and 189.1 ppm, respectively), indicating the presence of only one carbonyl group for each metabolite (data not shown). Together, these data point at glutathionyl adduct formation accompanied by H_2O adduct formation, both at the C ring of the fisetin *o*-quinone/quinone methide. The fact that two metabolites with similar MS, ^{1}H NMR, and ^{13}C NMR characteristics are observed points to formation of different (diastereo) isomers of these combined H_2O/glutathionyl adducts. A detailed further discussion on the structure of these fisetin metabolites is presented in the Discussion. Together, these results point to a reaction of the quinone/quinone methide of fisetin with glutathione which is surprisingly different from the chemistry observed for the other flavonoid quinones.

pH Dependence for formation of Glutathionylfisetin Adducts. Panels a−e of Figure 5 show the pH dependence for the formation of the glutathionylfisetin adducts. At lower pH values (≤7.0), the two major metabolites with retention times of 15.6 and 16.5 min are observed and the peak intensities of these metabolites decrease with increasing pH (Figure 5a−d). In addition, the formation of a new metabolite with a retention time of 22.1 min could be observed. At higher pH values (≥9.5), the two major metabolites formed at lower pH are no longer observed and the metabolite with a retention time of 22.1 min becomes the major metabolite (Figure 5e). The LC/MS analysis of this purified metabolite shows an M + 1 peak at *m*/*z* 592 (data not shown). Table 5 shows the ^{1}H NMR characteristics of this major metabolite collected from HPLC. Comparison of the ^{1}H NMR data of this metabolite to those of fisetin (Table 5) (*31*, *34*) reveals the loss of the H2′ signal as well as the loss of the $^4J_{H2'-H6'}$ coupling of 2.1 Hz. Splitting patterns and

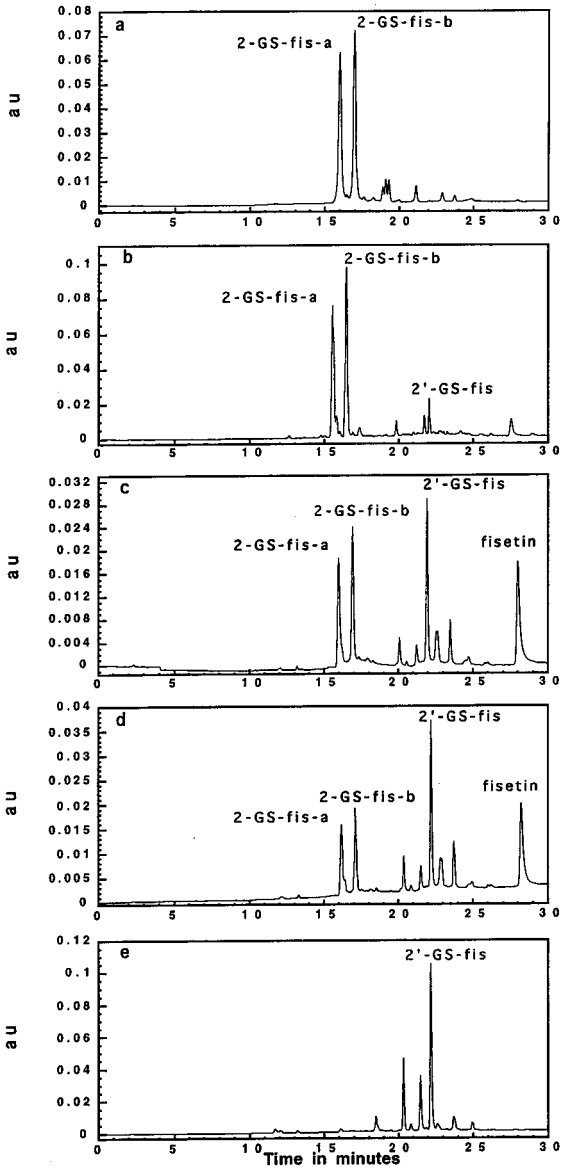

Figure 5. HPLC chromatograms of the incubation of fisetin with HRP in the presence of glutathione at pH (a) 3.5, (b) 7.0, (c) 8.5, (d) 9.0, and (e) 11.0.

resonances of all other aromatic protons are comparable to those of fisetin itself. In addition to the aromatic ^{1}H resonances, the ^{1}H NMR spectrum of the adduct exhibits the ^{1}H NMR resonances of the glutathionyl side chain. On the basis of these ^{1}H NMR characteristics and LC/MS data, the glutathionyl adduct can be identified as 2′-glutathionylfisetin resulting from conjugation in the B ring instead of in the C ring.

Calculation of the Chemical Reactivity toward Oxidation of the Studied 3′,4′-Dihydroxyflavonoids and Their Corresponding 2′-Glutathionyl Adducts. Table 6 presents the E_{HOMO} values and the relative differences in E_{HOMO} (ΔE_{HOMO}) of the studied 3′,4′-dihydroxyflavonoids and their corresponding 2′-glutathionyl adducts calculated using the semiempirical AM1 method. The results reveal that for luteolin the ease of oxidation of the parent compound and its corresponding 2′-glutathionyl adduct is almost the same and for taxifolin the oxidation of its corresponding 2′-glutathionyl adduct is even easier than of the parent compound.

Table 6. Calculated Energies of the Highest Occupied Molecular Orbital (E_{HOMO}) and the Relative Difference in E_{HOMO} of the Investigated 3′,4′-Dihydroxyflavonoids and Their 2′-Glutathionyl Adducts, Obtained with the AM1 Semiempirical Method

	E_{HOMO} (eV)		
compd	parent	2′-glutathionyl adduct	ΔE_{HOMO} (eV)
quercetin	−8.71	−8.97	−0.26
taxifolin	−8.91	−8.09	0.82
luteolin	−9.09	−9.18	−0.09
3,3′,4′-trihydroxyflavone	−8.65	−8.93	−0.28
fisetin	−8.65	−8.92	−0.27

Discussion

Quinone and quinone methides from a variety of natural and synthetic compounds, including 3′,4′-dihydroxyflavonoids and catechol-type metabolites from polycyclic aromatic hydrocarbons, estrogens, and compounds such as the anticancer drug tamoxifen, have been classified as likely candidates for reactive metabolites able to react with cellular macromolecules (*11*, *13*, *35*). For 3′,4′-dihydroxyflavonoids, with an intrinsic catechol moiety, their pro-oxidative quinone/quinone methide chemistry is especially important because of their increasing use as functional food ingredients and food supplements (*1*, *36*−*38*). Recently, the GSH trapping method (*19*−*21*) appeared to be an excellent method for investigating the quinone/quinone methide chemistry of the flavonoid quercetin (*22*, *23*), known to be mutagenic in a variety of bacterial and mammalian mutagenicity tests presumably through its quinone methide-like metabolites (*2*, *13*, *14*). The results of the study presented here, in which the quinone/quinone methide chemistry of an additional series of 3′,4′-dihydroxyflavonoids was investigated, provide new insight into the quinone/quinone methide chemistry of 3′,4′-dihydroxyflavonoids.

On the basis of the quinone/quinone methide isomerization chemistry involved in the formation of the A ring-type glutathionyl adducts from quercetin *o*-quinone/quinone methide (Figure 1), it can be postulated that especially the C2=C3 double bond, the C3−OH group, the C4-keto group, and the C5− and/or C7−OH group are required for efficient quinone methide formation and GSH adduct formation in the A ring instead of in the B ring. In the study presented here, this hypothesis was investigated in more detail.

The formation of 2′-glutathionyltaxifolin is in line with this hypothesis. Although saturation of the C2=C3 double bond, in theory, does not eliminate the quinone methide chemistry of the *o*-quinone of taxifolin to extend to the C ring, its conjugation with glutathione appears to be dominated by the *o*-quinone isomer, resulting in preferential GSH addition at C2′.

With luteolin which lacks the C3−OH group but still contains the C2=C3 double bond, glutathionyl adduct formation was observed preferentially at the C2′ position, giving rise to 2′-glutathionylluteolin. Elimination of the 3-OH prevents quinone methide isomerization since the rearrangement of the proton of the 3-OH group to generate a 3-keto group (Figure 1) can no longer occur. This restricts the structure of oxidized luteolin to the *o*-quinone isomer and, thus, the glutathione addition to the B ring (*14*, *39*). Preferential formation of 2′-glutathionylluteolin is in line with the preferential regioselectivity observed for glutathione conjugation of taxifolin *o*-quino-

ne. This observation is also in line with the calculations on the various theoretically possible glutathionyl adducts in the B ring of quercetin *o*-quinone, showing C2′ in the flavonoid *o*-quinone to be more reactive than C5′ or C6′ (*22*). Upon subsequent oxidation of both 2′-glutathionyllluteolin and 2′-glutathionyltaxifolin to their corresponding quinones, glutathione addition at C5′ is observed, resulting in formation of 2′,5′-diglutathionyl adducts. One may wonder about this tendency of especially 2′-glutathionylluteolin and 2′-glutathionyltaxifolin to compete with the parent flavonoid for HRP oxidation followed by glutathionyl adduct formation, since formation of diglutathionyl adducts was not observed as readily for any of the other 3′,4′-dihydroxyflavonoids. From time-dependent measurements with luteolin, it follows that especially when the concentration of the 2′-monoglutathionylluteolin reaches the residual concentration of luteolin itself, formation of the diadduct starts to compete. Thus, the discrepancy with respect to the ease of diglutathionyl adduct formation, observed to be relatively favored for especially luteolin and taxifolin, may best be ascribed to the relative tendency of HRP to oxidize the parent compound as opposed to the 2′-monoglutathionyl adduct. The reason 2′-glutathionylluteolin and 2′-glutathionyltaxifolin oxidation appears to be relatively efficient can be derived from molecular orbital calculations. For luteolin, the calculated ionization potential ($-E_{HOMO}$) and thus the ease of oxidation of the parent compound as compared to that of the 2′-glutathionyl adduct are almost the same (Table 6). For taxifolin, the calculated ionization potential reveals that the oxidation of 2′-glutathionyltaxifolin is even easier than the oxidation of the parent compound. This explains why especially for luteolin and taxifolin and not for the other model compounds of this study diglutathionyl adduct formation is readily observed.

With 3,3′,4′-trihydroxyflavone, the lack of the 5-OH group eliminates the intramolecular hydrogen bond of the 5-OH group to the 4-keto and results in formation of an alternative intramolecular hydrogen bond of the proton of the 3-OH group to the oxygen of the 4-carbonyl group (*14*, *39*). This hydrogen bond interaction of the 3-OH moiety has been reported to hamper the tautomerization of the 3-OH group to a 3-keto group and, thus, the formation of quinone methides (Figure 1). This explains why, upon elimination of the C5− and C7−OH moieties, glutathione conjugation is dominated by the *o*-quinone, resulting, as for luteolin and taxifolin, in the preferential formation of the 2′-glutathionyl adduct of 3,3′,4′-trihydroxyflavone.

Finally, the quinone/quinone methide trapping results of fisetin were different from what could be expected on the basis of the results with the other 3′,4′-dihydroxyflavonoids. The presence of the C2═C3 double bond and the C3−OH group but also the C7−OH group, in theory, may allow the quinoid structural element to extend to the A ring, resulting in the formation of quinone methide **I** (Figure 1) and providing possibilities for adduct formation at C6 and C8, as in the case of quercetin. However, as in 3,3′,4′-trihydroxyflavone, the lack of the 5-OH group might induce strong hydrogen bonding of the proton of the 3-OH group to the oxygen of the 4-carbonyl group (*14*, *39*), which, as for 3,3′,4′-trihydroxyflavone, would hamper the tautomeric shift of the *o*-quinone to the corresponding quinone methide (*14*) and would give rise to adduct formation in the B ring, leading to 2′-glutathionylfisetin as a major product. Surprisingly, fisetin quinone behaved quite different. Two adducts were formed which were shown to still contain all six aromatic fisetin protons; i.e., H5, H6, and H8 (A ring) and H2′, H5′, and H6′ (B ring) were all still present. This indicates that glutathione addition to fisetin quinone occurs in the C ring. Furthermore, the MS data reveal that both adducts, in addition to the glutathionyl moiety, also contain an additional *m/z* 18 which must be due to an additional H_2O moiety incorporated in the adduct. Especially this latter observation suggests that the reactivity of the fisetin quinone may be initially dominated by a type of reactivity reported previously also for the reaction of quercetin quinone with hydroxyl anions (*40*). This reactivity includes protonation of the quinone followed by hydroxyl (OH^-) attack at C2 in the C ring of the flavonoid quinone (Figure 6). This hydration results in 3,4-flavandione, **I**. In analogy with anthocyanins, a ring chain tautomeric equilibrium resulting in the chalcantrione, **II**, may exist, which subsequently may lead to formation of the substituted 3(2*H*)-benzofuranone, **III**. GS^- addition at C2 of **II** or **III** may result in formation of sets of two diastereoisomeric glutathionylfisetin adducts.

Clearly, ^{1}H NMR and MS data of these substituted 3(2*H*)-benzofuranones and/or chalcantriones are unable to discriminate between these possibilities, a problem reported previously for full identification of 3,4-flavandione (**I**)-derived additive products (*40*). However, ^{13}C NMR spectra which indicate the formation of two sp^3 resonances and one carbonyl group for each metabolite clearly reveal formation of the diastereoisomeric glutathionyl adducts of 3(2*H*)-benzofuranone (**V**) and not those of chalcantrione (**IV**) (Figure 6). Nevertheless, the data presented here for fisetin clearly illustrate two important new aspects of flavonoid quinone/quinone methide chemistry. First, the data provide an answer to the question of what causes the differential behavior of fisetin quinone as compared to the other flavonoid quinones with respect to preferential reactivity with water as compared to GS^- addition. Second, the data answer the question of what makes quercetin quinone react with the soft nucleophile GS^- at C6 and C8, but with water (H^+/OH^-) at C2. The results of this study clearly indicate that the answers to those questions can be found in the actual reaction conditions and subtle differences in pK_a of the various quinone/quinone methides causing differences in the tendency to actually initiate the protonation and OH^- addition pathway as an alternative for GS^- addition. Based on these considerations, Figure 6 gives possible pathways for the formation of the GS^-/OH^- adducts of fisetin *o*-quinone. These pathways explain the unexpected quinone/quinone methide chemistry observed in the study presented here. A competition exists between (i) the reaction of the quinone/quinone methide with the glutathionyl anion (GS^-) leading to A or B ring adducts and (ii) a protonation of the quinone/quinone methide leading to water addition as an early event. Differences in the flavonoid structure may be expected to influence this balance in a subtle way. Experiments on the pH-dependent glutathione adduct formation of fisetin confirm the hypothesis that with increasing pH, protonation of the quinone becomes more difficult, increasing the chances of direct glutathione adduct formation of the quinone in the B ring at C2′ as the preferential site for GS^- attack on the quinone. All together, the results of this study provide significant new

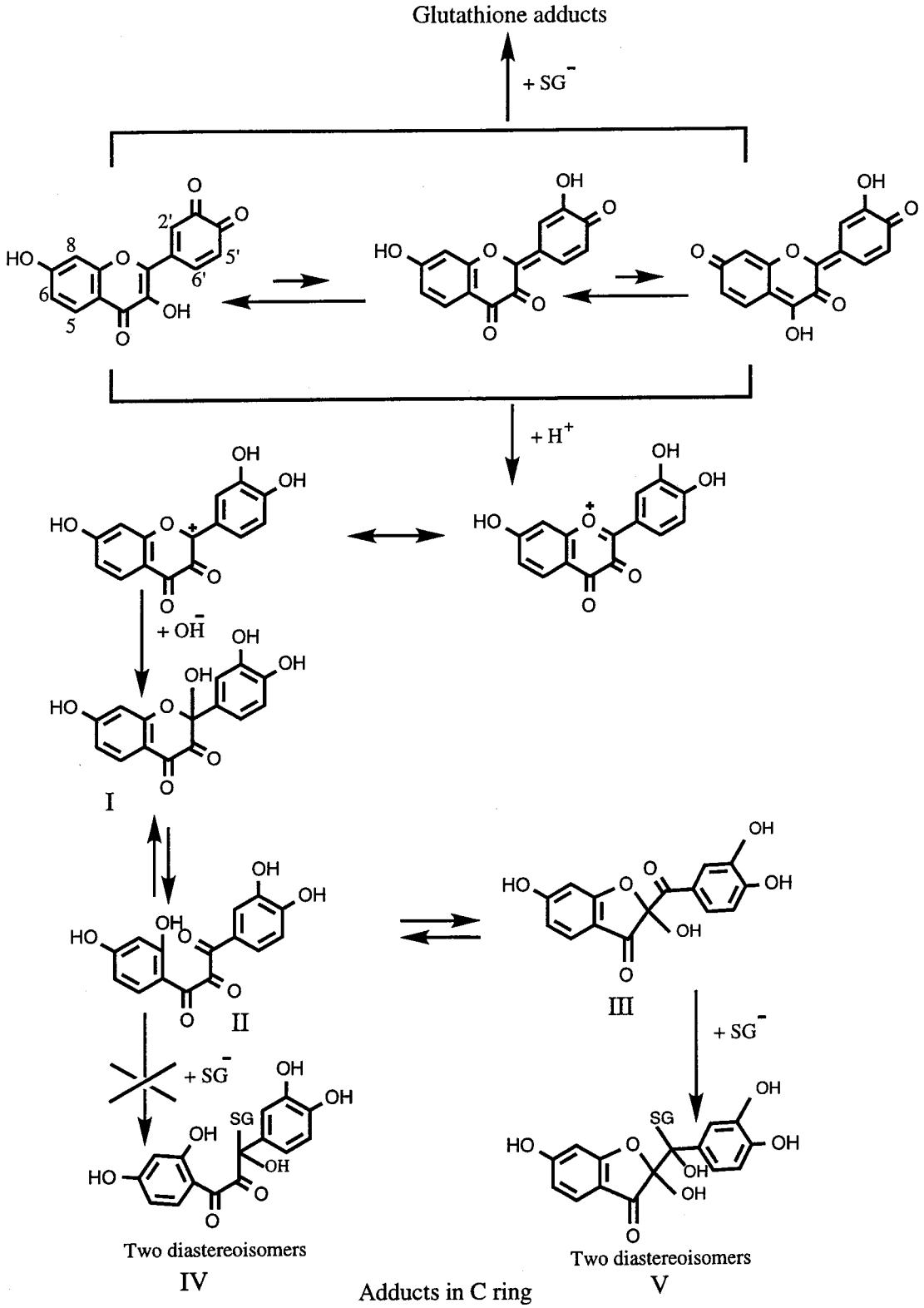

Figure 6. Hypothesis for the pH-dependent pathways for formation of the GS^-/OH^- adducts of fisetin *o*-quinone.

insight into the *o*-quinone/quinone methide chemistry of flavonoids and show the importance of the pH for the chemistry of this important class of electrophiles. This pH dependency of quercetin and other investigated flavonoids is presently under investigation.

This study identifies the nature of GSH conjugates of several flavonoid quinones. This opens the way for future studies aimed at investigating the formation of these GSH conjugates and their corresponding mercapturic acids in cellular in vitro and in vivo systems. The actual formation of these glutathionylflavonoid quinone adducts and of their corresponding mercapturic acids would represent an in vivo bioactivation pathway of these supposed beneficial functional food ingredients. The formation of quinone-derived mercapturic acids would be comparable to the formation of the glutathionyl and *N*-acetylcysteine conjugates of estrogens (*41*). Recently, *o*-quinones have been highlighted as active intermediates

in the development of cancer (*11*, *21*, *41*−*45*), since the presence of *o*-quinone−DNA complexes has been confirmed (*11*, *43*, *44*). It has been demonstrated that the *o*-quinones of estrogens react with glutathione, producing *N*-acetylcysteine conjugates in an in vitro system using rat liver (*46*, *47*). In addition, it has been suggested that the urinary levels of mercapturate can be used as a biomarker for exposure to active nucleophilic materials (*48*−*50*). Thus, it might be meaningful to determine the urinary levels of these *N*-acetylcysteine conjugates as markers of quinone-induced tumorigenesis. However, the actual detection of these conjugates in urine, for example, requires sensitive detection methods and knowledge of the stability, nature, and chemical behavior of the adducts. The results of this present study indicate the nature of the adducts that should be expected upon (auto)oxidation of a series of flavonoids and provide a basis for the future detection of their mercapturic acids in biological samples as possible markers of pro-oxidative flavonoid behavior and toxicity in vivo.

Acknowledgment. We gratefully acknowledge support by EU Grant ERBFMGECT 950066 (large-scale facility Wageningen NMR Centre) and by a grant from the Graduate School of Environmental Chemistry and Toxicology (M&T). H.M.A. is grateful to her Egyptian supervisors, Dr. Ahmed M. Shalaby and Dr. Mohamed H. Abo-Ghalia, for continuous support.

References

(1) Jovanovic, S. V., Steenken, S., Tosic, M., Marjanovic, B., and Simic, M. G. (1994) Flavonoids as antioxidants. *J. Am. Chem. Soc.* **116**, 4846−4851.

(2) Middleton, E., Jr., and Kandaswami, C. (1993) The impact of plant flavonoids on mammalian biology: Implications for immunity, inflammation and cancer. In *The Flavonoids: Advances in Research Since 1986* (Harborne, J. H., Ed.) pp 619−652, Chapman and Hall, New York.

(3) Cody, V., Middleton, E., and Harborne, J. B. (1986*) Plant Flavonoids in Biology and Medicine: Biochemical Pharmacological and Structure−Activity Relationships,* A. R. Liss, New York.

(4) Rice-Evans, C. A., Miller, N. J., and Paganga, G. (1996) Structure antioxidant activity relationships of flavonoids and phenolic acids. *Free Radical Biol. Med.* **20**, 933−956.

(5) Manach, C., Regerat, F., Texier, O., Agullo, G., Demigne, C., and Remesy, C. (1996) Bioavailability, metabolism and physiological impact of flavonoids. *Nutr. Res.* **16**, 517−544.

(6) Salah, N., Miller, N. J., Paganga, G., Tyburg, L., Bolwell, G. P., and Rice-Evans, C. (1995) Polyphenolic flavonols as scavengers of aqueous phase radicals and chain-breaking antioxidants. *Arch. Biochem. Biophys.* **322**, 339−346.

(7) Yamanaka, N., Oda, O., and Nagao, S. (1997) Prooxidant activity of caffeic acid, dietary non-flavonoid phenolic acid, on Cu^{2+}-induced low-density lipoprotein oxidation. *FEBS Lett.* **405**, 186−190.

(8) Laughton, M. J., Halliwell, B., Evans, P. J., and Hoult, J. R. S. (1989) Antioxidant and prooxidant actions of the plant phenolics quercetin, gossypol and myricetin. *Biochem. Pharmacol.* **38**, 2859−2865.

(9) Metodiewa, D., and Dunford, H. B. (1993) Medical aspects and techniques for peroxidases and catalases. In *Atmospheric Oxidation and Antioxidants* (Scott, G., Ed.) Vol. III, pp 287−332, Elsevier, Amsterdam.

(10) Metodiewa, D., Jaiswal, A. K., Cenas, N., Dickancaite, E., and Segura-Aguilar, J. (1999) Quercetin may act as a cytotoxic prooxidant after its metabolic activation to semiquinone and quinoidal product. *Free Radical Biol. Med.* **26**, 107−116.

(11) Bolton, J. L., Pisha, E., Zhang, F., and Qiu, S. (1998) Role of quinoids in estrogen carcinogenesis. *Chem. Res. Toxicol.* **11**, 1113−1126.

(12) Penning, T. M., Burczynski, M. E., Hung, C. F., McCoull, K. D., Palackal, N. T., and Tsuruda, L. S. (1999) Dihydrodiol dehydrogenases and polycyclic aromatic hydrocarbon activation: generation of reactive and redox active *o*-quinones. *Chem. Res. Toxicol.* **12**, 1−18.

(13) Murty, V. S., and Penning, T. M. (1992) Polycyclic aromatic hydrocarbon (PAH) *ortho*-quinone conjugate chemistry: kinetics of thiol addition to PAH *ortho*-quinones and structures of thioether adducts of naphthaline-1,2-dione. *Chem.-Biol. Interact.* **84**, 169−188.

(14) MacGregor, J. T., and Jurd, L. (1978) Mutagenicity of plant flavonoids: structural requirements for mutagenic activity in *Salmonella typhimurium*. *Mutat. Res.* **54**, 297−309.

(15) Bolton, J. L., and Shen, L. (1996) *p*-Quinone methides are the major decomposition products of catechol estrogen *o*-quinones. *Carcinogenesis* **17**, 925−929.

(16) Galati, G., Chan, T., Wu, B., and O'Brien, P. J. (1999) Glutathione-dependent generation of reactive oxygen species by the peroxidase-catalysed redox cycling of flavonoids. *Chem. Res. Toxicol.* **12**, 521−525.

(17) O'Brien, P. J. (1988) Radical formation during the peroxidase-catalysed metabolism of carcinogens and xenobiotics: the reactivity of these radicals with GSH, DNA and unsaturated lipid. *Free Radical Biol. Med.* **4**, 169−183.

(18) Sudhar, P. S., and Armstrong, D. A. (1990) Redox potential of some sulfer containing radicals. *J. Phys. Chem.* **94**, 5915−5917.

(19) Butterworth, M., Lau, S. S., and Monks, T. J. (1996) 17-β-Estradiol metabolism by hamster hepatic microsomes: Comparison of catechol estrogen O-methylation with catechol estrogen oxidation and glutathione conjugation. *Chem. Res. Toxicol.* **9**, 793−799.

(20) Iverson, S. L., Shen, L., Anlar, N., and Bolton, J. L. (1996) Bioactivation of estrone and its catechol metabolites to quinoid-glutathione conjugates in rat liver microsomes. *Chem. Res. Toxicol.* **9**, 492−499.

(21) Butterworth, M., Lau, S. S., and Monks, T. J. (1997) Formation of catechol estrogen glutathione conjugates and γ-glutamyl transpeptidase-dependent nephrotoxicity of 17-β-estradiol in the golden Syrian hamster. *Carcinogenesis* **18**, 561−567.

(22) Awad, M. H., Boersma, M. G., Vervoort, J., and Rietjens, I. M. C. M. (2000) Peroxidase-catalysed formation of quercetin quinone methide glutathione adducts. *Arch. Biochem. Biophys.* **378**, 224−233.

(23) Boersma, M. G., Vervoort, J., Szymusiak, H., Lemanska, K., Tyrakowska, B., Cenas, N., Segura-Aguilar, J., and Rietjens, I. M. C. M. (2000) Regioselectivity and reversibility of the glutathione conjugation of quercetin quinone methide. *Chem. Res. Toxicol.* **13**, 185−191.

(24) Primus, J.-L., Boersma, M. G., Mandon, D., Boeren, S., Veeger, C., Weiss, R., and Rietjens, I. M. C. M. (1999) The effect of iron to manganese substitution on microperoxidase 8 catalysed peroxidase and cytochrome P450 type of catalysis. *J. Biol. Inorg. Chem.* **4**, 274−283.

(25) Osman, A. M., Koerts, J., Boersma, M. G., Boeren, S., Veeger, C., and Rietjens, I. M. C. M. (1996) Microperoxidase/H_2O_2-catalysed aromatic hydroxylation proceeds by cytochrome-P-450-type oxygen-transfer reaction mechanism. *Eur. J. Biochem.* **240**, 232−238.

(26) Stoll, V. C., and Blanchard, J. S. (1990) Buffers: Principles and practice. *Methods Enzymol.* **182**, 24−38.

(27) Dewar, M. J. S., Zoebisch, E. G., Healy, E. F., and Stewart, J. J. P. (1985) AM1: A new general purpose quantum mechanical molecular model. *J. Am. Chem. Soc.* **107**, 3902−3909.

(28) Rietjens, I. M. C. M., Soffers, A. E. M. F., Hooiveld, G., Veeger, C., and Vervoort, J. (1995) Quantitative structure activity relationships (QSAR's) based on computer calculated parameters for the overall rate of glutathione S-transferase catalysed conjugation of a series fluoronitrobenzenes. *Chem. Res. Toxicol.* **8**, 481−488.

(29) Zheng, Y. J., and Ornstein, R. L. (1997) Mechanism of nucleophilic aromatic substitution of 1-chloro-2,4-dinitrobenzene by glutathione in the gas phase and in solution. Implication for the mode of action of glutathione S-transferase. *J. Am. Chem. Soc.* **119**, 648−655.

(30) Zheng, Y. J., and Ornstein, R. L. (1997) Role of active site tyrosine in glutathione S-transferase: insight from a theoretical study on model systems. *J. Am. Chem. Soc.* **119**, 1523−1528.

(31) Corazza, A., Harvey, I., and Sadler, P. J. (1996) H-1, C-13-NMR and X-ray absorption studies of copper(I) glutathione complexes. *Eur. J. Biochem.* **236**, 697−705.

(32) Markham, K. R., and Geiger, H. (1993) ^{1}H NMR magnetic resonance spectroscopy of flavonoids and their glycosides in hexadeuterodimethylsulfoxide. In *The Flavonoids: Advances in Research Since 1986* (Harborne, J. H., Ed.) pp 619−652, Chapman and Hall, London.

(33) Youssef, D., and Frahm, A. W. (1995) Constituents of the Egyptian *Centaurea scoparia*. III. Phenolic constituents of the aerial parts. *Planta Med.* **61**, 570−573.

(34) Aksnes, D. W., Standnes, A., and Andersen, O. M. (1996) Complete assignment of the ^{1}H and ^{13}C NMR spectra of flavone and its A-ring hydroxyl derivatives. *Magn. Reson. Chem*. **34**, 820−823.
(35) Zhang, F., Fan, P. W., Liu, X., Shen, L., van Breemen, R., and Bolton, J. L. (2000) Synthesis and reactivity of a potential carcinogenic metabolite of tamoxifen: 3,4-Dihydroxytamoxifen-*o*-quinone. *Chem. Res. Toxicol*. **13**, 53−62.
(36) Espin, J. C., Morales, M., Varon, R., Tuleda, J., and Garcia-Canovas, F. (1995) A continuous spectrophotometric method for determining the monophenolase and diphenolase activities of apple polyphenol oxidase. *Anal. Biochem*. **231**, 237−246.
(37) Espin, J. C., Tuleda, J., and Garcia-Canovas, F. (1998) 4-Hydroxyanisole: the most suitable monophenolic substrate for determining spectrophotometrically the monophenolase activity of polyphenol oxidase from fruits and vegetables. *Anal. Biochem*. **259**, 118−126.
(38) Shahar, T., Henning, N., Gutfinger, T., Hareven, D., and Lifschitz, E. (1992) The Tomato 66.3 kDa polyphenoloxidase gene: molecular identification and developmental expression. *Plant Cell* **4**, 135−147.
(39) Dean, F. M. (1963) *Naturally occurring oxygen ring compounds*, p 285, Butterworths, London.
(40) Jorgensen, L. V., Cornett, C., Justesen, U., Skibsted, L. H., and Dragsted, L. O. (1998) Two-electron electrochemical oxidation of quercetin and kaempferol changes only the flavonoid C-ring. *Free Radical Res.* **29**, 339−350.
(41) Nakagomi, M., and Suzuki, E. (2000) Quantitation of catechol estrogens and their n-Acetylcysteine conjugates in urine of rats and hamsters. *Chem. Res. Toxicol.* **13**, 1208−1213.
(42) Zhu, B. T., and Conney, A. H. (1998) Functional role of estrogen metabolism in target cells: review and perspectives. *Carcinogenesis* **19**, 1−27.
(43) Cavalieri, E. L., Stack, D. E., Devanesan, P. D., Todorovic, R., Dwivedy, I., Higginbotham, S., Johansson, S. L., Patil, K. D., Gross, M. L., Gooden, J. K., Ramanathan, R., Cerny, R. L., and Rogan, E. G. (1997) Molecular origin of cancer: Catechol estrogen-3,4-quinones as endogenous tumor initiators. *Proc. Natl. Acad. Sci. U.S.A.* **94**, 10937−10942.
(44) Akanni, A., and Abul-Hajj, Y. J. (1997) Estrogen-nucleic acid adducts. Reaction of 3,4-estrone *o*-quinone with nucleic acid bases. *Chem. Res. Toxicol*. **10**, 760−766.
(45) Liehr, J. G. (1997) Hormone-associated cancer: Mechanistic similarities between human breast cancer and estrogen-induced kidney carcinogenesis in hamsters. *Environ. Health Perspect*. **105** (Suppl. 3), 565−569.
(46) Kuss, E. (1971) Mikrosomale oxidation des oestradiol-17B (Microsomal oxidation of estradiol-17B). *Hoppe-Seyler's Z. Physiol. Chem*. **352**, 817−836.
(47) Elce, J. S. (1970) Metabolism of glutathione conjugate of 2-hydroxyestradiol by rat liver and kidney preparations in vitro. *Biochem. J*. **116**, 913−917.
(48) Suzuki, E., Osabe, M., Okada, M., Ishizaki, T., and Suzuki, T. (1987) Urinary metabolites of *N*-nitrosodibutylamine and *N*-nitrodibutylamine in the rat: Identification of *N*-acetyl-*S*-alkyl cysteines. *Jpn. J. Cancer Res*. **78**, 382−385.
(49) Vermeulen, N. P. E. (1989) Analysis of mercapturic acids as a tool in biotransformation, biomonitoring and toxicological studies. *Trends Pharmacol. Sci*. **10**, 177−181.
(50) Boogaard, P. J., and van Sittert, N. J. (1996) Suitability of S-phenyl mercapturic acid and trans-trans-muconic acid as biomarkers for exposure to low concentrations of benzene. *Environ. Health Perspect*. **104**, 1151−1157.

TX000216E